Chinese Chemical Letters 35 (2024) 109692

Contents lists available at ScienceDirect

Chinese Chemical Letters

journal homepage: www.elsevier.com/locate/cclet

Alkyl chain engineering of boron dipyrromethenes for efficient photodynamic antibacterial treatment

Qihang Wu[a,b], Hui Wen[a,b], Wenhai Lin[c,*], Tingting Sun[a,*], Zhigang Xie[a,b,*]

[a] State Key Laboratory of Polymer Physics and Chemistry, Changchun Institute of Applied Chemistry, Chinese Academy of Sciences, Changchun 130022, China
[b] School of Applied Chemistry and Engineering, University of Science and Technology of China, Hefei 230026, China
[c] Biomedical Polymers Laboratory, College of Chemistry, Chemical Engineering and Materials Science, and State Key Laboratory of Radiation Medicine and Protection, Soochow University, Suzhou 215123, China

ARTICLE INFO

Article history:
Received 29 December 2023
Revised 4 February 2024
Accepted 29 February 2024
Available online 5 March 2024

Keywords:
BODIPY
Alkyl chain engineering
Photodynamic therapy
Antibacterial agent
Photosensitizer

ABSTRACT

Photodynamic therapy has been widely employed as an alternative strategy against bacterial infection. Molecular structure has a profound effect on the antibacterial ability of photosensitizers (PSs). Herein, we designed and synthesized a series of boron dipyrromethene (BODIPY)-based photosensitizers with different alkyl chain lengths, and then their antibacterial activities were compared. Among these BODIPYs, the BODIPY with octyl (BDP-8) exhibits the best antibacterial effect, while the antibacterial performance of BODIPY with dodecyl (BDP-12) is the worst. This work provides instructive information for further development of effective photodynamic antimicrobial agents.

Bacterial infection seriously threatens human health [1–3]. Particularly, the abuse of antibiotics causes bacterial drug resistance, which makes antibacterial treatment more intractable [4–6]. Therefore, it is necessary and urgent to develop alternative strategies to combat bacterial infection. As an emerging treatment strategy, photodynamic therapy (PDT) utilizes photosensitizers (PSs) under irradiation to generate reactive oxygen species (ROS) [7–10]. PDT is initially employed to kill tumor cells *via* the toxic ROS [11–13], but recently it has attracted great attention as an alternative antibacterial strategy [14–18]. Compared with the traditional treatments like antibiotics, PDT hardly causes bacterial drug resistance because the oxidative damage of ROS to bacteria involves a multi-target damage process [19–21]. However, the short lifespan and the limited effective distance of ROS severely restrict their antibacterial performance [22–24]. Interestingly, introducing targeting groups such as cationic groups to PSs could enhance the interactions between the PSs and bacteria, which dramatically improve their antibacterial effects [25–27].

The interactions between the antibacterial agents and bacteria can also be fine-tuned by the subtle structural differences [28–30]. For instance, the lengths of alkyl chains of molecules play an important role in tuning their hydrophobic interactions with bacteria and other living organisms [31,32]. The influence of the lengths of alkyl chains on the performance of antibacterial agents has been explored in previous works [33–35]. For example, Xu's group has revealed the relationship between the molecular sizes of ionic liquid derivatives and their antibacterial abilities [36]. However, the effect of the alkyl chain length on the antibacterial ability of PSs has less been studied.

Boron dipyrromethene (BODIPY), as a promising PS, has been widely studied for photodynamic anticancer and antibacterial treatments due to its high extinction coefficient, satisfactory photostability and chemical stability, as well as high tunability of photophysical properties [37–39]. In this work, BODIPY is selected as the PS, and alkyl chains with different lengths (ethyl, butyl, hexyl, octyl, and dodecyl) are introduced to the pyridyl on the *meso* position of BODIPYs, which are named BDP-2, BDP-4, BDP-6, BDP-8, and BDP-12, respectively (Scheme 1). Under green light irradiation, these BODIPYs possess nearly the same ability of ROS generation. However, their antibacterial performance is not stronger and stronger with the lengths of alkyl chains increased as we expect. The BODIPY with octyl (BDP-8) exhibits the best antibacterial effect against either *Staphylococcus aureus (S. aureus)* or *Escherichia coli (E. coli)*.

The synthetic route of BODIPYs with different alkyl chain lengths are shown in Fig. 1a. The synthesis of BDP-Py and IBDP-Py refers to the reported methods [40,41]. The molecular structures of BDP-2, BDP-4, BDP-6, BDP-8, and BDP-12 are validated by nuclear magnetic resonance (^{1}H and ^{13}C NMR) spectroscopy (Figs. S1-S5 in Supporting information) and mass spectrometry (Figs. S6-S10 in

* Corresponding authors.
E-mail addresses: whlin@suda.edu.cn (W. Lin), suntt@ciac.ac.cn (T. Sun), xiez@ciac.ac.cn (Z. Xie).

https://doi.org/10.1016/j.cclet.2024.109692
1001-8417/

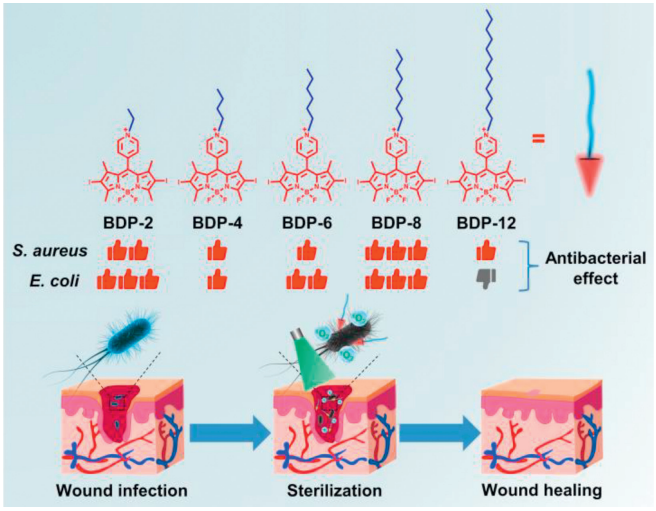

Scheme 1. The molecular structures of BODIPYs and comparisons of their antibacterial effects.

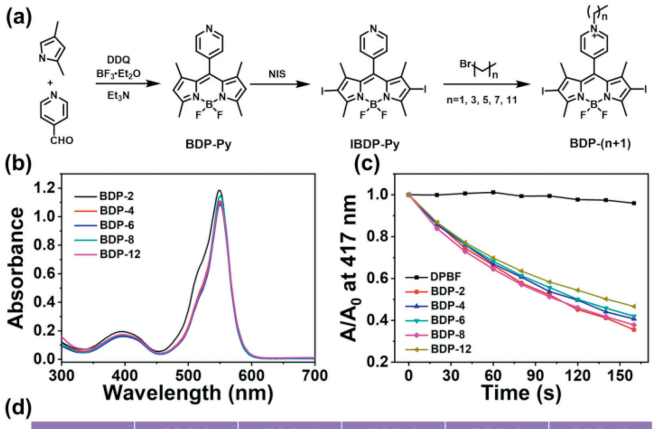

	BDP-2	BDP-4	BDP-6	BDP-8	BDP-12
S_1 (eV)	1.17	1.22	1.24	1.25	1.25
T_1 (eV)	1.06	1.11	1.11	1.10	1.11
ΔE_{ST} (eV)	0.11	0.10	0.13	0.15	0.14

Fig. 1. (a) The synthetic route of BODIPYs (BDP-2, BDP-4, BDP-6, BDP-8, and BDP-12). (b) Absorption spectra of BODIPYs. (c) ROS generation of BODIPYs (1 μmol/L) under light irradiation over time detected *via* DPBF. (d) ΔE_{ST} (S_1-T_1) of BODIPYs calculated by DFT.

Supporting information). Besides, the C–H vibration bands of $-CH_2$ at 2853 cm^{-1} are observed in the Fourier-transform infrared (FTIR) spectra of BDP-2, BDP-4, BDP-6, BDP-8, and BDP-12, further implying the successful synthesis of BODIPYs with different alkyl chain lengths (Fig. S11 in Supporting information).

Next, the absorption and emission spectra of these BODIPYs were measured. As shown in Fig. 1b and Fig. S12 (Supporting information), similar absorption and emission spectra at the same concentration were observed. To compare their photodynamic activities, 1,3-diphenylisobenzofuran (DPBF) was employed to detect the production of ROS upon green light irradiation. As displayed in Fig. 1c and Fig. S13 (Supporting information), the absorbance at 417 nm of DPBF incubated with BDP-2, BDP-4, BDP-6, BDP-8, and BDP-12 decreases rapidly with the increase of irradiation time, while that of DPBF alone changes slightly. More importantly, there is no obvious difference among the variation ranges of their absorbance, showing that these BODIPYs possess similar ability of ROS generation. Besides, the singlet-triplet energy gaps (ΔE_{ST}) of BDP-2, BDP-4, BDP-6, BDP-8, and BDP-12 are calculated *via* density

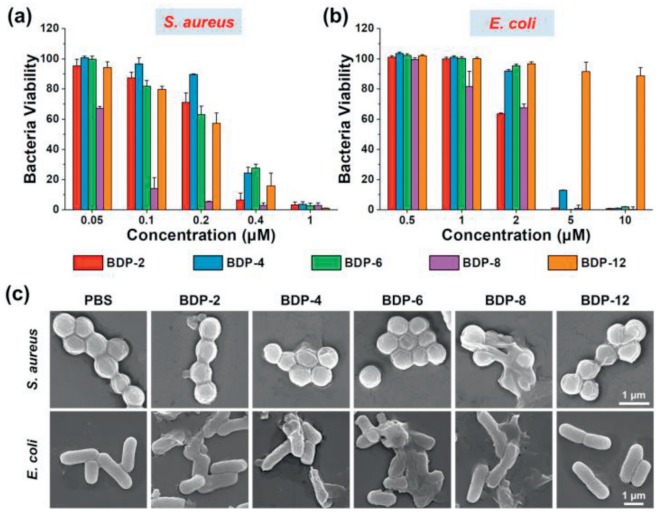

Fig. 2. Bacterial viability of (a) *S. aureus* and (b) *E. coli* treated with different concentrations of BDP-2, BDP-4, BDP-6, BDP-8, or BDP-12 and green light irradiation (18 mW/cm^2). (c) SEM images of *S. aureus* and *E. coli* treated with BODIPYs and green light irradiation.

functional theory (DFT). As shown in Fig. 1d, there is not much difference in their ΔE_{ST}, which further suggests that the lengths of the introduced alkyl chains have insignificant influence on the ability of ROS generation of the BODIPY agents.

To compare the ROS generation efficiency of BODIPYs, we chose BDP-8 as a representative and Rose Bengal (a commercial photosensitizer similar to Acid Red 94) for comparison. As shown in Fig. S14 (Supporting information), under the same conditions, the absorbance of DPBF incubated with BDP-8 decreases at a similar rate with that treated with Rose Bengal with the increase of irradiation time, indicating that they possess similar ROS generation efficiency. Furthermore, to investigate the specific type of ROS generated by these BODIPYs (BDP-8 as a representative), 9,10-anthracenediyl-bis(methylene)-dimalonic acid (ABDA) and dihydrorhodamine 123 (DHR 123) were selected as the indicators of singlet oxygen ($^1O_2$) and superoxide anion radicals ($O_2^{\cdot-}$) respectively. As shown in Fig. S15 (Supporting information), the absorbance of ABDA incubated with BDP-8 decreases rapidly with the increase of irradiation time, indicating that BDP-8 exposed to light irradiation could generate $^1O_2$. Meanwhile, the FL intensity of DHR 123 treated with BDP-8 increased rapidly with prolonged irradiation time (Fig. S16 in Supporting information), indicating the generation of $O_2^{\cdot-}$ by BDP-8. Results above suggest these BODIPYs could generate both $^1O_2$ and $O_2^{\cdot-}$ under light irradiation.

To compare their antibacterial performance, *S. aureus* and *E. coli* were chosen as the representatives of Gram-positive and Gram-negative bacteria respectively. Surprisingly, under light irradiation, BDP-8 exhibits the best antibacterial performance against *S. aureus*, and the antibacterial effect of BDP-2 against *S. aureus* is second to that of BDP-8. While BDP-4, BDP-6, and BDP-12 show similar antibacterial ability, which is lower than that of BDP-2 and BDP-8 (Fig. 2a). For *E. coli*, BDP-2 and BDP-8 possess the best antibacterial effect under light irradiation, while BDP-12 exhibits the worst antibacterial performance. The antibacterial effect of BDP-4 and BDP-6 is second to that of BDP-2 and BDP-8 (Fig. 2b). Above all, among the 5 BODIPYs under irradiation, BDP-8 exerts the best antibacterial ability against either *S. aureus* or *E. coli*. Furthermore, the antibacterial performance of these BODIPYs under dark condition was further investigated. As shown in Fig. S17a (Supporting information), these BODIPYs at a low concentration (1 μmol/L) in the absence of light irradiation exhibit insignificant toxicity against *S. aureus*, though different degrees of dark toxicity can be observed

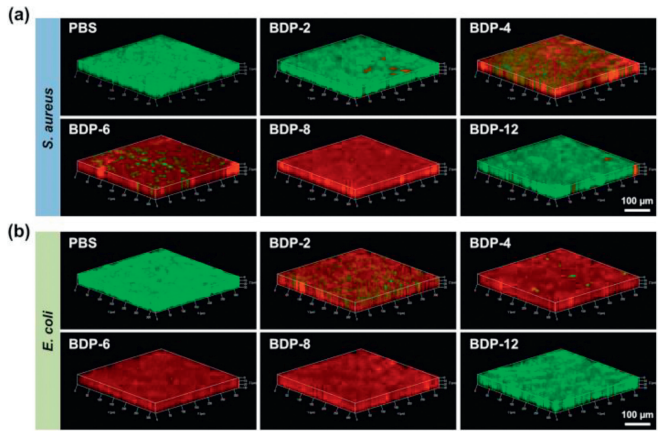

Fig. 3. Antibiofilm performance of BODIPYs toward (a) *S. aureus* and (b) *E. coli* biofilms under green light irradiation.

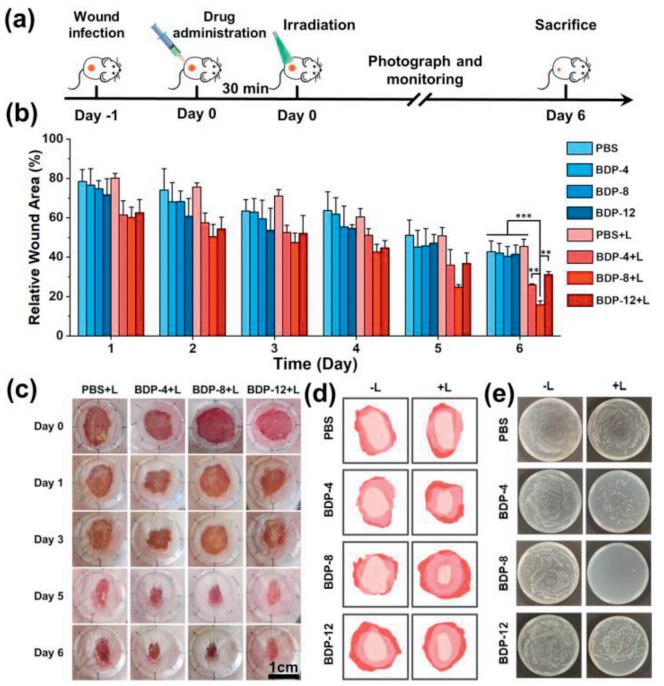

Fig. 4. (a) Schematic illustration of the process of wound healing experiment. (b) Changes of the wound areas in each group after different treatments. $^{**}P < 0.01$ and $^{***}P < 0.001$. (c) Photos of the wounds in the groups of PBS+L, BDP-4 + L, BDP-8 + L, and BDP-12+L after treatments for different time. (d) Schematic diagram of the wound areas during the healing process. (e) Photographs of the bacteria separated from the wound tissues in agar plates.

for BODIPYs at higher concentrations. As for *E. coli*, these BODIPYs at a high concentration of 10 μmol/L without irradiation still exhibit insignificant toxicity (Fig. S17b in Supporting information).

To further compare their bactericidal effect, we observed the morphology changes of bacteria treated with BODIPYs and light irradiation *via* scanning electron microscopy (SEM). As displayed in Fig. 2c, the membranes of the *S. aureus* treated with BDP-8 or BDP-2 are damaged, while those treated with BDP-4, BDP-6, or BDP-12 are still intact. Similarly, the *E. coli* treated with BDP-8 show the most severe membrane lysis and leakage of cytoplasm. These results further verify that there is obvious difference among the antibacterial activities of different BODIPYs. Since the BODIPYs possess the same fluorophore core and positive charge, we speculate that the distinctions in antibacterial effect mainly attribute to the hydrophobic interactions between BODIPYs with different alkyl chain lengths and bacteria. Long alkyl chain could cause physical damage of bacteria by inserting into the bacterial membrane, while too long alkyl chain such as that of BDP-12 may curl and thus cover the positive charge located in the pyridyl group, which may block the electrostatic interaction between the PS and bacteria [42].

Due to the protection of extracellular polymeric substances, biofilm is more difficult to be eliminated than bacterioplankton. Therefore, the antibiofilm ability of BODIPYs toward *S. aureus* and *E. coli* biofilms was investigated. First, we studied the ROS generation of BODIPYs in the biofilms with 2′,7′-dichlorodihydrofluorescein diacetate (DCFH-DA, 10 μmol/L) as the fluorescence probe. As shown in Fig. S18 (Supporting information), the biofilms incubated with BODIPYs under light irradiation exhibit strong green fluorescence, implying that all of these BODIPYs could generate ROS in the biofilms. There is no significant difference in the fluorescence intensity among these green images, which suggests that the BODIPYs have similar ability of ROS generation in biofilms.

Then, the eradication effect of BODIPYs under light irradiation toward biofilms was investigated *via* three-dimensional confocal laser scanning microscopy (3D CLSM). As displayed in Fig. 3a, the *S. aureus* biofilm incubated with BDP-8 exhibits strong red fluorescence (dead bacteria stained with PI), while that treated with BDP-2 or BDP-12 shows bright green fluorescence (live bacteria stained with SYTO). For the *E. coli* biofilms, after incubation with BDP-6 or BDP-8, similar and strong red fluorescence was observed, while intense green fluorescence was presented for that treated with BDP-12 (Fig. 3b). The above results indicate that BDP-8 could almost completely kill the bacteria in the biofilms, while BDP-12 possesses negligible toxicity to the bacteria in the biofilms. The antibiofilm ability of the other three BODIPYs is between that of BDP-8 and BDP-12.

To compare the antibacterial effect of BODIPYs *in vivo*, we established wound infection model of female Kunming mice and selected BDP-4, BDP-8, as well as BDP-12 as the representatives. The whole experimental process is illustrated in Fig. 4a. 24 h after being infected with *E. coli*, the wounds were treated with BODIPYs and then irradiated with green light. The wound healing of the mice was monitored by photographing the wounds and calculating the wound sizes. As shown in Fig. 4b, the wound areas gradually decrease over time, and the wounds treated with BDP-8 and light irradiation (BDP-8 + L) possess the minimum relative wound area on the 6th day. Moreover, the wound healing rate of the wounds in BDP-12+L group is 68.9%, worse than that of the wounds in the groups of BDP-4 + L (74.1%) and BDP-8 + L (84.2%). As shown in the photographs of the wounds in Fig. 4c, Figs. S19 and S20 (Supporting information), the wounds in the group of BDP-8 + L exhibit the best wound healing effect. The process of wound healing in each group could be visually seen in Fig. 4d.

The mice were sacrificed after 6 days of treatments, and the wound tissues were cut off. After that, the bacteria were separated from the wound tissues *via* ultrasonication, and then cultured on the agar plates. As shown in Fig. 4e, there are a lot of bacterial colonies in the groups of PBS, PBS+L, BDP-4, BDP-8, and BDP-12, while few bacteria exist in BDP-8 + L group. Moreover, the number of bacteria colonies in BDP-8 + L group is much less than that in BDP-4 + L and BDP-12+L groups. The wound tissues were also stained with hematoxylin and eosin (H&E). There are a mass of inflammatory cells and incomplete epidermis in PBS group, while newly grown epidermis and few inflammatory cells are observed in BDP-8 + L group (Fig. S21 in Supporting information). Results above indicate that the combination of BDP-8 and light irradiation exhibit the best antibacterial effect and wound healing performance.

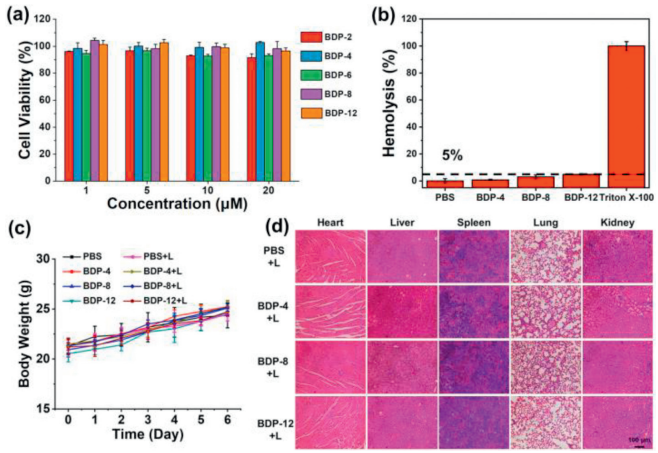

Fig. 5. (a) Cell viability of L929 cells treated with 5 BODIPYs at different concentrations without light irradiation (Mean ± SD, $n = 3$). (b) Hemolysis ratios of BDP-4, BDP-8, and BDP-12 (Triton X-100 as the positive control) (Mean ± SD, $n = 3$). (c) Body weight changes of the mice in each group during the therapeutic process (Mean ± SD, $n = 4$). (d) Images of major organs stained with H&E.

To study the cytotoxicity of BODIPYs, mouse fibroblast (L929) and mouse embryonic fibroblast (NIH 3T3) cells were employed to conduct 3-(4,5-dimethylthiazol-2-yl)−2,5-diphenyltetrazolium bromide (MTT) assays. As shown in Fig. 5a and Fig. S22 (Supporting information), 5 BODIPYs possess insignificant cytotoxicity even at a high concentration (20 μmol/L). Next, hemolysis test of BDP-4, BDP-8, and BDP-12 was carried out. Their hemolysis ratios gradually increase with the lengths of alkyl chains increased (Fig. 5b), but they are all at a safe level (below 5%) [43]. In the wound healing experiment, the mice in all groups kept gaining weight steadily during the treatments (Fig. 5c), suggesting that these BODIPYs have no obvious systemic toxicity in the therapeutic concentration range. Besides, their major organs were stained with H&E after the mice were sacrificed. As displayed in Fig. 5d, no significant abnormity of organ sections is found in the groups of BDP-4 + L, BDP-8 + L, and BDP-12+L, indicating their good biosafety.

To conclude, we designed and synthesized a series of BODIPY-based PSs with different alkyl chain lengths. These BODIPYs exhibit similar ability of ROS generation. Surprisingly, their antibacterial ability does not get stronger and stronger with the alkyl chain length increased. Among the 5 BODIPYs, BDP-8 with octyl exhibits the best antibacterial effect against both gram-positive (*S. aureus*) and gram-negative (*E. coli*) bacteria *in vitro* experiments, while BDP-12 with dodecyl exhibits the worst antibacterial effect, probably because the long alkyl chain curls and thus covers the positive charge located in the pyridyl group. The experiment of wound infection further verifies the admirable antibacterial ability and effect of BDP-8 in promoting wound healing. This work provides a new perspective on the influence of the alkyl chain lengths on the antibacterial effect of PSs and useful information toward further exploration of antimicrobial agents.

Declaration of competing interest

The authors declare no conflict of interest.

Acknowledgment

The authors greatly acknowledge the financial support from the National Natural Science Foundation of China (Nos. 52003267 and 51973214).

Supplementary materials

Supplementary material associated with this article can be found, in the online version, at doi:10.1016/j.cclet.2024.109692.

References

[1] A. Cassini, L.D. Högberg, D. Plachouras, et al., Lancet Infect. Dis. 19 (2019) 56–66.
[2] P.C. Ray, S.A. Khan, A.K. Singh, D. Senapati, Z. Fan, Chem. Soc. Rev. 41 (2012) 3193–3209.
[3] D.L. Heymann, Cell 124 (2006) 671–675.
[4] M.F. Richter, B.S. Drown, A.P. Riley, et al., Nature 545 (2017) 299–304.
[5] B. Tse Sum Bui, T. Auroy, K. Haupt, Angew. Chem. Int. Ed. 61 (2022) e202106493.
[6] B. Hu, C. Owh, P.L. Chee, et al., Chem. Soc. Rev. 47 (2018) 6917–6929.
[7] J. Xu, Y. Lai, F. Wang, et al., Chin. Chem. Lett. 34 (2023) 108332.
[8] Z. Wang, Y. Jiang, Q. Zhang, et al., Sens. Actuator. B 401 (2024) 135072.
[9] W. Zhu, Y. Li, S. Guo, et al., Nat. Commun. 13 (2022) 7046.
[10] B. Zhang, L. Lin, J. Mao, et al., Chin. Chem. Lett. 34 (2023) 108518.
[11] J.C.H. Chu, C.T.T. Wong, D.K.P. Ng, Angew. Chem. Int. Ed. 62 (2023) e202214473.
[12] Q. Sun, Q. Su, Y. Gao, et al., Aggregate 4 (2023) e298.
[13] L. Wang, A. Mei, N. Li, et al., Chin. Chem. Lett. 35 (2024) 108974.
[14] M.L. Agazzi, M.B. Ballatore, A.M. Durantini, E.N. Durantini, A.C. Tomé, J. Photochem. Photobiol. C 40 (2019) 21–48.
[15] J. Gong, L. Liu, C. Li, et al., Chem. Sci. 14 (2023) 4863–4871.
[16] C. Li, Y. Li, Q. Wu, T. Sun, Z. Xie, Biomater. Sci. 9 (2021) 7648–7654.
[17] K. Cheng, H. Wang, S. Sun, et al., Small 19 (2023) 2207868.
[18] H. Zhang, C. He, L. Shen, et al., Chin. Chem. Lett. 34 (2023) 108160.
[19] F. Cieplik, D. Deng, W. Crielaard, et al., Crit. Rev. Microbiol. 44 (2018) 571–589.
[20] B. Ran, Y. Yuan, W. Xia, et al., Chem. Sci. 12 (2020) 1054–1061.
[21] E. Alves, M.A.F. Faustino, M.G. Neves, et al., Future Med. Chem. 6 (2014) 141–164.
[22] L. Jiang, C.R.R. Gan, J. Gao, X.J. Loh, Small 12 (2016) 3609–3644.
[23] C. Hopper, Lancet Oncol. 1 (2000) 212–219.
[24] P. Du, Y. Shen, B. Zhang, et al., Adv. Sci. 10 (2023) 2206851.
[25] H. Zhang, Q. Li, X. Qi, et al., Chem. Eng. J. 451 (2023) 138261.
[26] H. Chen, S. Li, M. Wu, et al., Angew. Chem. Int. Ed. 59 (2020) 632–636.
[27] Y. Yu, Y. Liu, Y. Chen, et al., J. Mater. Chem. Front. 7 (2023) 96–105.
[28] R.J. Bingham, P. Ballone, J. Phys. Chem. B 116 (2012) 11205–11216.
[29] Z. Zheng, Q. Xu, J. Guo, et al., ACS Appl. Mater. Interfaces 8 (2016) 12684–12692.
[30] N. Nikfarjam, M. Ghomi, T. Agarwal, et al., Adv. Funct. Mater. 31 (2021) 2104148.
[31] A. Busetti, D.E. Crawford, M.J. Earle, et al., Green Chem. 12 (2010) 420–425.
[32] L. Guo, C. Li, H. Shang, R. Zhang, et al., Chem. Sci. 11 (2020) 661–670.
[33] T. Guo, X. Wang, Y. Shu, J. Wang, J. Mol. Liq. (2021) 339.
[34] Z. Zhuang, Z. Meng, J. Li, et al., ACS Nano 16 (2022) 11912–11930.
[35] N. Li, Y.Y. Liu, Y. Li, et al., ACS Appl. Mater. Interfaces 10 (2018) 24249–24257.
[36] L. Zheng, J. Li, M. Yu, et al., J. Am. Chem. Soc. 142 (2020) 20257–20269.
[37] H.B. Cheng, X. Cao, S. Zhang, et al., Adv. Mater. 35 (2023) 2207546.
[38] X. Xing, E. Pang, S. Zhao, et al., Chin. Chem. Lett. 35 (2024) 108467.
[39] X. Chen, B.B. Mendes, Y. Zhuang, et al., J. Am. Chem. Soc. 146 (2024) 1644–1656.
[40] S. Banfi, G. Nasini, S. Zaza, E. Caruso, Tetrahedron 69 (2013) 4845–4856.
[41] M.K. Raza, S. Gautam, P. Howlader, et al., Inorg. Chem. 57 (2018) 14374–14385.
[42] F. Li, M.D. Weir, H.H. Xu, J. Dent. Res. 92 (2013) 932–938.
[43] G.P. Yang, X.L. Meng, S.J. Xiao, et al., ACS Appl. Mater. Interfaces 14 (2022) 28289–28300.